Journal of Medicinal Chemistry

Article

pubs.acs.org/jmc

Novel ^{18}F-Labeled Benzoxazole Derivatives as Potential Positron Emission Tomography Probes for Imaging of Cerebral β-Amyloid Plaques in Alzheimer's Disease

Mengchao Cui,[†,‡] Masahiro Ono,[†,*] Hiroyuki Kimura,[†] Masashi Ueda,[†,§] Yuji Nakamoto,[§] Kaori Togashi,[§] Yoko Okamoto,[∥] Masafumi Ihara,[∥] Ryosuke Takahashi,[∥] Boli Liu,[‡] and Hideo Saji[†]

[†]Department of Patho-Functional Bioanalysis, Graduate School of Pharmaceutical Sciences, Kyoto University, 46-29 Yoshida Shimoadachi-cho, Sakyo-ku, Kyoto 606-8501, Japan

[‡]Key Laboratory of Radiopharmaceuticals, Ministry of Education, College of Chemistry, Beijing Normal University, Beijing 100875, PR China

[§]Department of Diagnostic Imaging and Nuclear Medicine, Graduate School of Medicine, Kyoto University, 54 Shogoin Kawahara-cho, Sakyo-ku, Kyoto 606-8507, Japan

[∥]Department of Neurology, Graduate School of Medicine, Kyoto University, 54 Shogoin Kawahara-cho, Sakyo-ku, Kyoto 606-8507, Japan

Supporting Information

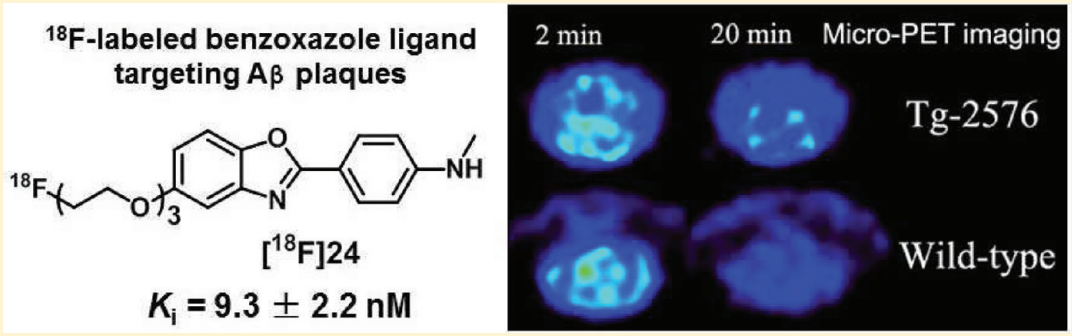

ABSTRACT: Two radiofluoro-pegylated phenylbenzoxazole derivatives, 4-(5-(2-(2-(2-[^{18}F]fluoroethoxy)ethoxy)ethoxy)benzo-[*d*]oxazol-2-yl)-*N*-methylaniline ([^{18}F]**24**) and 4-(5-(2-(2-(2-[^{18}F]fluoroethoxy)ethoxy)ethoxy)benzo[*d*]oxazol-2-yl)-*N*,*N*-dimethylaniline ([^{18}F]**32**), were synthesized and evaluated as probes for imaging cerebral β-amyloid (Aβ) plaques in living brain tissue by PET. [^{18}F]**24** and [^{18}F]**32** displayed high affinity for Aβ_{1-42} aggregates (K_i = 9.3 and 3.9 nM, respectively). In vitro autoradiography with sections of post-mortem AD brain and transgenic mouse brain confirmed the affinity of these tracers. Initial high uptake into and rapid washout from the brain in normal mice were observed. [^{18}F]**24** also displayed excellent binding to Aβ plaques in ex vivo autoradiographic experiments with Tg2576 mice. Furthermore, small-animal PET studies demonstrated significant differences in the clearance profile after the administration of [^{18}F]**24** between Tg2576 and wild-type mice. The results suggest [^{18}F]**24** to be a useful PET agent for detecting Aβ plaques in the living human brain.

INTRODUCTION

Dementia is the third most common cause of death after cancer and cardiac vascular disorders, and Alzheimer's disease (AD) is the most common form of dementia, characterized by progressive memory impairment, disordered cognitive functions, altered behavior, and a decline in language function. The pathological hallmarks of AD are extracellular deposits of β-amyloid (Aβ) plaques and intracellular neurofibrillary tangles (NFTs).[1−3] Currently, the clinical diagnosis of AD is only a probable diagnosis and a histological diagnosis can only be obtained after death. According to the amyloid cascade hypothesis, amyloid deposits constitute a central and initial event in the pathogenesis of AD. Therefore, a tracer agent for positron emission tomography (PET) that specifically binds to these Aβ plaques will provide an important tool for the noninvasive in vivo diagnosis of AD.[4,5] Furthermore, it might also be used to predict the development of AD before the onset of dementia and to assess the effect of antiamyloid therapy.[6]

The search for small, neutral, and moderately lipophilic imaging agents targeting Aβ plaques in the living human brain has been extensive (Figure 1). Among PET probes investigated in the past decade, a thioflavin-T derivative, [^{11}C]-2-(4-(methylamino)phenyl)-6-hydroxybenzothiazol ([^{11}C]**1**: PIB),

Special Issue: Alzheimer's Disease

Received: February 24, 2012
Published: June 12, 2012

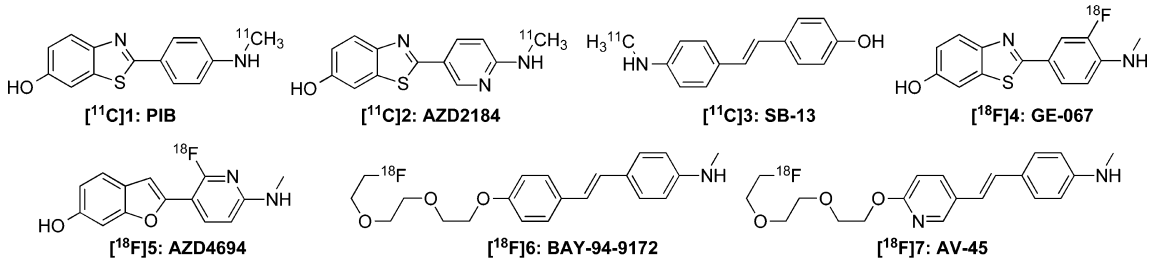

Figure 1. Chemical structure of PET imaging agents targeting Aβ plaques in AD patients.

is the most suitable and most extensively studied. PET studies indicate that AD and control cases can be clearly distinguished by using [^{11}C]**1**.[7−9] Recently, Andersson et. al reported a close analogue of PIB, [^{11}C]-2-[6-(methylamino)pyridin-3-yl]-1,3-benzothiazol-6-ol ([^{11}C]**2**: AZD2184), which has the positive attributes of [^{11}C]**1** but with an apparent lower degree of nonspecific binding in white matter. Preliminary human PET studies suggested that [^{11}C]**2** displayed favorable brain kinetics and an excellent contrast for Aβ plaques in the brain of AD patients.[10−12] Beside the core structure of thioflavin-T, the stilbene scaffold has also been selected for developing Aβ imaging agents. The first ^{11}C-labeled stilbene derivative was [^{11}C]-4-*N*-methylamino-4′-hydroxystilbene ([^{11}C]**3**: SB-13): PET imaging in vivo with [^{11}C]**3** demonstrated potential usefulness in detecting Aβ plaques in the human brain.[13,14] However, the routine clinical use of ^{11}C-labeled tracers is limited by the short half-life of ^{11}C ($T_{1/2}$ = 20 min). Additional tracers labeled with the radionuclide ^{18}F ($T_{1/2}$ = 110 min, 511 keV, commonly produced by a cyclotron) would be more useful for PET.

Thus, a [^{11}C]**1** analogue, [^{18}F]-2-(3-fluoro-4-methyaminophenyl)benzothiazol-6-ol ([^{18}F]**4**: GE-067),[15] and a [^{11}C]**2** derivative, [^{18}F]-2-(2-fluoro-6-(methylamino)pyridin-3-yl)benzofuran-6-ol ([^{18}F]**5**: AZD4694),[16] are currently under phase II clinical testing in Europe. Preliminary studies in AD patients suggested that they may potentially be useful for PET imaging of Aβ plaque burden in living brain tissue. At the same time, two stilbene derivatives with a short length of polyethylene glycol units (PEG, n = 3), [^{18}F]-4-(*N*-methylamino)-4′-(2-(2-(2-fluoroethoxy)ethoxy)ethoxy)-stilbene ([^{18}F]**6**: BAY94−9172)[4,17] and [^{18}F]-(*E*)-4-(2-(6-(2-(2-(2-fluoroethoxy)ethoxy)ethoxy)pyridin-3-yl)vinyl)-*N*-methylaniline ([^{18}F]**7**: AV-45)[18−20] are under commercial development.

In an attempt to develop more promising amyloid imaging agents, we chose to investigate benzofuran derivatives designed to be isosteric analogues of thioflavin-T (Figure 2). Initially, we prepared a series of radioiodinated benzofuran derivatives ([^{125}I]**8**−**11**), which displayed excellent affinity for Aβ_{1-40} aggregates (K_i = 0.4−9.0 nM). However, limited penetration of the brain (<1.5%ID after an iv injection in normal mice) together with nonspecific binding made them unsuitable for imaging plaques in vivo.[21] With additional structural changes, we then obtained a ^{11}C-labeled benzofuran derivative ([^{11}C]**13**) with improved properties.[22] More recently, we have reported a series of novel fluorinated pyridylbenzofuran and phenylbenzofuran derivatives ([^{18}F]**14**−**17**) with polyethylene glycol side chains as potential ^{18}F-labeled tracers for the imaging of Aβ plaques by PET.[23,24] These ligands showed high affinity for Aβ_{1-42} aggregates in vitro and for Aβ plaques in sections of autopsied AD brain. Compared with the dimethylated [^{18}F]**14** and [^{18}F]**15**, [^{18}F]**16** and [^{18}F]**17** with a monomethylamino group exhibited greater initial uptake into the brain. The pyridylbenzofuran derivative [^{18}F]**16** provided the best pharmacokinetics of radioactivity in the brain, the $\text{brain}_{2\ \text{min}}/\text{brain}_{60\ \text{min}}$ ratio being 2.34. In addition, ex vivo autoradiograms indicated that [^{18}F]**16** showed selective binding of Aβ plaques with little nonspecific binding in the Tg2576 mouse brain.[25] Compared with the radioiodinated benzofuran derivatives, these fluoro-pegylated benzofuran derivatives had greatly improved pharmacokinetics.

A radioiodinated benzoxazole derivative, [^{125}I]-2-(4′-dimethylaminophenyl)-6-iodobenzoxazole ([^{125}I]**12**: IBOX), which is another close thioflavin-T analogue (Figure 2), displayed high affinity for Aβ_{1-40} aggregates in vitro (K_i = 0.8 nM).[26] Similar to that observed with radioiodinated benzofuran derivatives, [^{125}I]**12** displayed low brain uptake and high nonspecific binding. To improve the pharmacokinetic profile of [^{125}I]**12** for use as a PET imaging agent, the highly lipid soluble iodine atom was replaced by a short fluorine end-capped polyethylene glycol chain (n = 3). In addition, compared with the structure of benzofuran, the nitrogen atom in the oxazole ring would reduce the lipophilicity of the probe, thus reducing nonspecific binding and enhancing the signal-to-noise ratio. After this modification, the in vivo pharmacokinetic profile of the benzoxazole derivatives may be better than that of benzofuran derivatives. Here, we report the synthesis and biological evaluation of two novel fluoro-pegylated phenylbenzoxazole derivatives as PET probes for the detection of cerebral Aβ plaques in vivo.

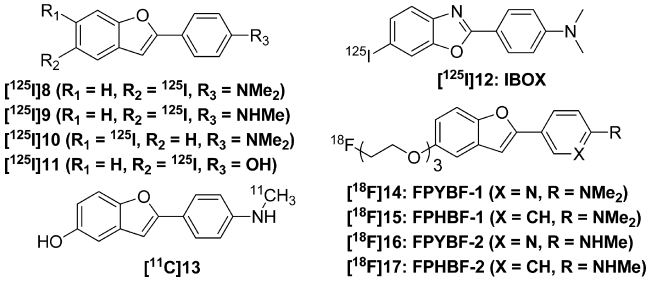

Figure 2. Chemical structure of radio-labeled benzofuran and benzoxazole derivatives reported previously.

RESULTS AND DISCUSSION

Chemistry and Radiochemistry. The synthesis of **24** and **32** is outlined in Schemes 1 and 2, respectively. The desired benzoxazoles (**20** and **28**) were obtained by a condensation reaction between 2-amino-4-methoxyphenol (**19**) and 4-monomethylaminobenzoic acid or 4-dimethylaminobenzoic acid catalyzed by polyphosphoric acid in yields of 31% and 25%, respectively. The *O*-methyl groups of **20** and **28** were removed by reacting with BBr_3 in CH_2Cl_2 to give **21** and **29** in

dx.doi.org/10.1021/jm300251n | J. Med. Chem. 2012, 55, 9136−9145

Scheme 1[a]

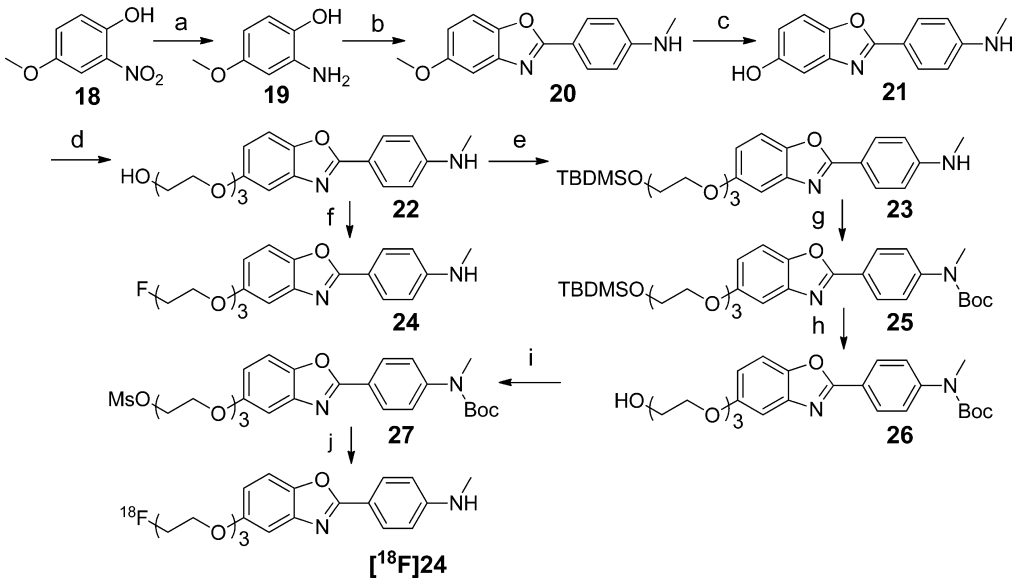

[a]Reagents and conditions: (a) Pd/C, MeOH, rt; (b) 4-methylaminobenzoic acid, PPA, 180°C; (c) BBr_3 (1 M in CH_2Cl_2), CH_2Cl_2, −78 °C to rt; (d) 2-[2-(2-chloroethoxy)ethoxy]ethanol, K_2CO_3, DMF, 110°C; (e) TBDMSCl, imidazole, CH_2Cl_2, rt; (f) DAST, CH_2Cl_2, −78 °C to rt; (g) $(Boc)_2O$, THF, reflux; (h) TBAF (1 M in THF), THF, rt; (i) MsCl, Et_3N, CH_2Cl_2, rt; (j) (1) $^{18}F^-$, K_2CO_3, Kryptofix-2.2.2, acetonitrile, 120 °C, (2) HCl (1 M), 120 °C.

Scheme 2[a]

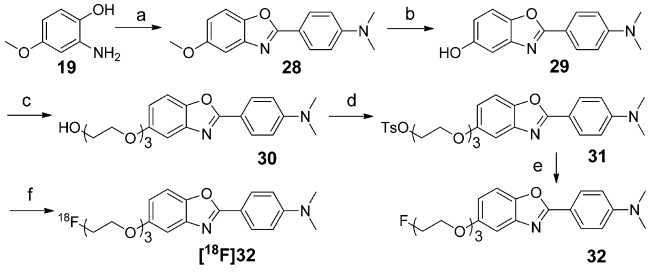

[a]Reagents and conditions: (a) 4-(dimethylamino)benzoic acid, PPA, 180 °C; (b) BBr_3 (1 M in CH_2Cl_2), CH_2Cl_2, −78 °C to rt; (c) 2-[2-(2-chloroethoxy)ethoxy]ethanol, K_2CO_3, DMF, 110 °C; (d) TsCl, pyridine, rt; (e) TBAF (1 M in THF), THF, reflux; (f) $^{18}F^-$, K_2CO_3, Kryptofix-2.2.2, acetonitrile, 120 °C.

yields of 91% and 88%, respectively. To prepare compounds with three ethoxy units as the polyethylene glycol linkage, 2-[2-(2-chloroethoxy)ethoxy]ethanol was coupled with the hydroxy groups of **21** and **29** to obtain **22** and **30**. For the monomethylated compound, the free hydroxy group in **22** was subsequently protected with *tert*-butyldimethylsilyl chloride (TBDMSCl) to give **23**. Compound **25** was obtained by protecting the methylamino group of **23** with a butyloxycarbonyl (BOC) group. After removal of the TBS-protected group of **25**, the free hydroxy group of **26** was converted into mesylates by reacting with methanesulfonyl chloride in the presence of triethylamine to give **27**. The fluorinated compound **24** was successfully obtained by stirring **22** and diethylaminosulfur trifluoride (DAST) in CH_2Cl_2 (Scheme 1). For the dimethylated compound, tosylation of the free hydroxyl group present in **30** afforded the precursor **31**, which readily reacted with anhydrous tetra-*n*-butylammonium fluoride (TBAF) at reflux to give the fluorinated compound **32** (Scheme 2).

The radiofluorinated ligands [^{18}F]**24** and [^{18}F]**32** were prepared from the corresponding mesylate or tosylate precursors (Schemes 1 and 2) with radiochemical yields of 30% and 60%, respectively. After purification by high performance liquid chromatography (HPLC), the radiochemical purity of these radiotracers was greater than 98%, and their specific activity was estimated as approximately 200 GBq/μmol. The identity of [^{18}F]**24** and [^{18}F]**32** was verified by a comparison of the retention time with that of the nonradioactive compound (see Supporting Information).

Biological Evaluation. *In Vitro Binding of **24** and **32** to Synthetic Aβ Aggregates.* The affinity of **24** and **32** for Aβ_{1-42} aggregates was examined in solutions with competition binding assays using [^{125}I]2-(4-dimethylaminophenyl)-6-iodoimidazo-[1,2-*a*]pyridine ([^{125}I]IMPY) as the competing radioligand.[27] Well-known Aβ imaging probes, IMPY[28,29] and PIB,[6,7] were also screened using the same system for comparison. The data in Table 1 demonstrate that they compete strongly with

Table 1. Inhibition Constants for the Binding of [^{125}I]IMPY to Aβ(1−42) Aggregates

compd	K_i (nM)[a]
24	9.3 ± 2.2
32	3.9 ± 0.7
IMPY	10.5 ± 1.0[b]
PIB	9.0 ± 1.3[b]

[a]Values are the means ± standard errors of the mean of three independent determinations. [b]Data from ref 25.

[^{125}I]IMPY for binding to Aβ_{1-42} aggregates (K_i = 9.3 and 3.9 nM, respectively). In addition, the affinity of these benzoxazole derivatives was comparable to the value for IMPY and PIB under the same assay conditions.

*Autoradiography of Transgenic Mouse Brain and Post-Mortem Brain Tissue Sections with [^{18}F]**24** or [^{18}F]**32**.* The

dx.doi.org/10.1021/jm300251n | J. Med. Chem. 2012, 55, 9136−9145

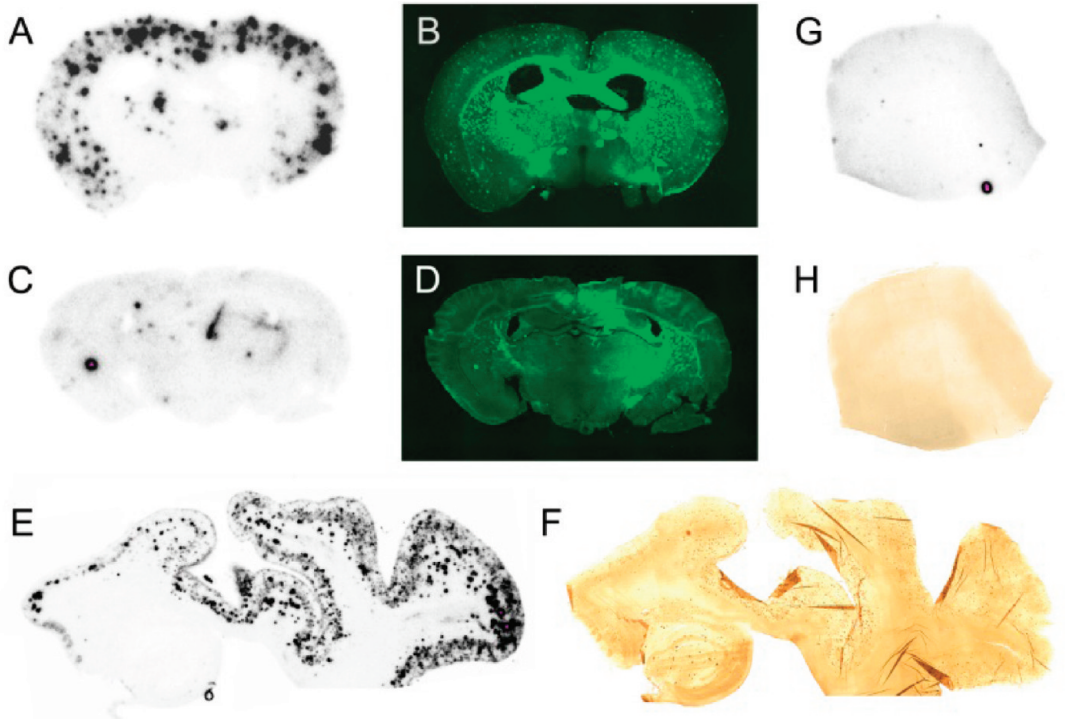

Figure 3. Autoradiography of [^{18}F]**24** in vitro in mouse brain sections ((A) Tg mouse, C57BL6, APPswe/PSEN1, 12 months old; (C) wild-type, C57BL6, 12 months old) and human brain sections ((E) AD, 93 years old, female; (G) normal, 71 years old, male). The presence and distribution of plaques in the sections were confirmed with thioflavin-S (B, D) and immunohistochemical staining using a monoclonal Aβ antibody (F, H).

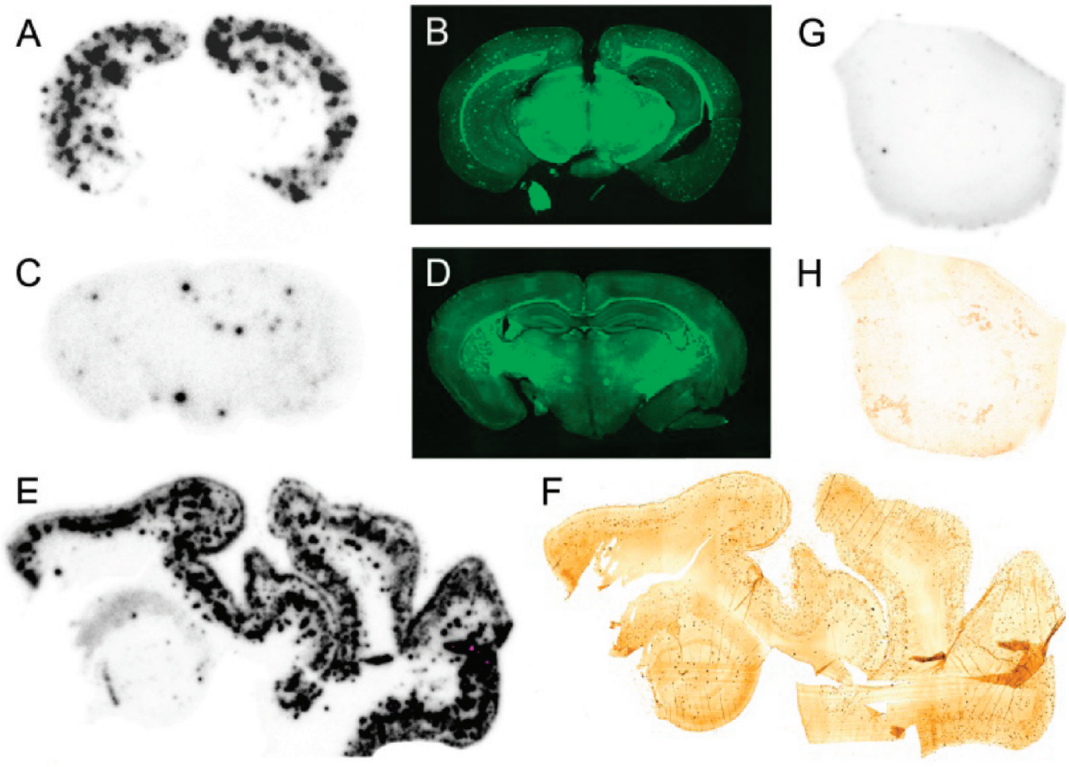

Figure 4. Autoradiography of [^{18}F]**32** in vitro in mouse brain sections ((A) Tg mouse, C57BL6, APPswe/PSEN1, 12 months old; (C) wild-type, C57BL6, 12 months old) and human brain sections ((E) AD, 93 years old, female; (G) normal, 71 years old, male). The presence and distribution of plaques in the sections were confirmed with thioflavin-S (B, D) and immunohistochemical staining using a monoclonal Aβ antibody (F, H).

high binding of the radiolabeled tracers ([^{18}F]**24** and [^{18}F]**32**) to Aβ plaques was further confirmed by in vitro autoradiography in sections of brain tissue from AD patients or Tg model mice (C57BL6, APPswe/PSEN1, 12 months old). As shown in Figures 3A and 4A, specific labeling of plaques was observed in the brain sections of transgenic mice. The

dx.doi.org/10.1021/jm300251n | *J. Med. Chem.* 2012, 55, 9136−9145

Table 2. Biodistribution in Normal ddY Mice after iv Injection of [^{18}F]**24**[a] and the Lipophilicity (log *D*) of the Ligand

[^{18}F]**24** (log *D* = 3.09 ± 0.05)				
organ	2 min	10 min	30 min	60 min
blood	4.76 ± 0.23	3.46 ± 0.26	4.67 ± 0.09	4.87 ± 0.24
brain	8.12 ± 0.51	4.41 ± 0.28	4.07 ± 0.07	3.04 ± 0.16
bone	3.17 ± 0.32	2.32 ± 0.20	3.74 ± 0.30	5.78 ± 0.53
heart	8.57 ± 0.51	4.78 ± 0.53	4.84 ± 0.35	4.32 ± 0.49
liver	20.28 ± 2.18	23.15 ± 2.85	19.31 ± 2.23	13.06 ± 1.41
spleen	3.90 ± 0.20	4.22 ± 0.67	3.92 ± 0.32	3.42 ± 0.49
lung	8.18 ± 0.92	5.64 ± 0.89	5.30 ± 0.36	5.22 ± 0.45
kidney	12.88 ± 0.56	8.45 ± 1.02	6.84 ± 0.55	5.40 ± 0.74
stomach[b]	1.59 ± 0.16	2.36 ± 1.16	1.85 ± 0.41	1.87 ± 0.27
intestine	11.33 ± 0.83	25.00 ± 3.96	23.92 ± 4.78	23.91 ± 8.84

[a]Expressed as % injected dose per gram. Average for 5 mice ± standard deviation. [b]Expressed as % injected dose per organ.

Table 3. Biodistribution in Normal ddY Mice after iv Injection of [^{18}F]**32**[a] and the Lipophilicity (log *D*) of the Ligand

[^{18}F]**32** (log *D* = 3.45 ± 0.09)				
organ	2 min	10 min	30 min	60 min
blood	3.24 ± 0.25	2.26 ± 0.12	2.84 ± 0.13	3.33 ± 0.41
brain	5.29 ± 0.19	3.37 ± 0.21	2.50 ± 0.20	2.12 ± 0.08
bone	1.18 ± 0.19	1.07 ± 0.31	1.96 ± 0.26	3.45 ± 0.31
heart	5.55 ± 0.53	3.52 ± 0.16	3.14 ± 0.18	3.13 ± 0.31
liver	13.04 ± 1.31	11.36 ± 1.10	9.20 ± 0.99	6.92 ± 0.66
spleen	3.60 ± 0.30	2.88 ± 0.51	2.53 ± 0.06	2.25 ± 0.37
lung	5.18 ± 0.23	3.64 ± 0.48	3.28 ± 0.22	3.22 ± 0.36
kidney	8.71 ± 0.96	5.18 ± 0.36	4.08 ± 0.35	3.68 ± 0.80
stomach[b]	1.10 ± 0.13	1.37 ± 0.52	1.51 ± 0.16	1.41 ± 0.34
intestine	4.80 ± 0.79	15.70 ± 1.51	22.59 ± 2.94	15.82 ± 1.67

[a]Expressed as % injected dose per gram. Average for 5 mice ± standard deviation. [b]Expressed as % injected dose per organ.

Table 4. Comparison of Inhibition Constants (K_i, nM) and Brain Kinetics between Radiofluorinated Benzoxazole Derivatives and Other Probes

tracers	K_i (nM)	2 min[a]	60 min[a]	ratio$_{2\ min/60\ min}$	log *D*
[^{18}F]**24**	9.5 ± 1.3	8.12 ± 0.51	3.04 ± 0.16	2.67	3.09
[^{18}F]**32**	3.9 ± 0.2	5.29 ± 0.19	2.12 ± 0.08	2.50	3.45
[^{125}I]**12**	0.8 ± 0.2	1.43 ± 0.23[b]	1.26 ± 0.10[b]	1.13	2.09
[^{18}F]**7**	2.87 ± 0.17	7.33 ± 1.54	1.88 ± 0.14	3.90	2.41
[^{18}F]**14**	1.0 ± 0.2	5.16 ± 0.30	2.44 ± 0.36	2.11	2.32
[^{18}F]**15**	2.0 ± 0.5	2.88 ± 0.46	2.80 ± 0.06	1.03	2.94
[^{18}F]**16**	2.4 ± 0.1	7.38 ± 0.84	3.15 ± 0.10	2.34	3.11
[^{18}F]**17**	3.9 ± 0.2	8.18 ± 0.59	3.87 ± 0.42	2.11	3.73

[a]Expressed as % injected dose per gram. [b]Expressed as % injected dose per organ.

distribution of Aβ plaques was consistent with the results of fluorescent staining with thioflavin-S, a dye commonly used for staining the Aβ plaques in human brain sections. (Figures 3B and 4B). As expected, highly dense labeling of plaques was observed in the brain sections of AD (Figures 3E and 4E). Immunohistochemical staining confirmed the presence of plaques in these sections (Figures 3F and 4F). In contrast, no apparent labeling was observed in wild-type mice and normal adult brain sections.

In Vivo Biodistribution in Normal ddY Mice. One prerequisite for a successful imaging agent for Aβ plaques in the brain is the ability to penetrate the BBB. It should also have fast washout kinetics in normal brain.[4] Therefore, the ability of [^{18}F]**24** and [^{18}F]**32** to penetrate the blood−brain barrier (BBB) was evaluated in vivo in normal ddY mice. As shown in Tables 2 and 3, both [^{18}F]**24** and [^{18}F]**32** exhibited good penetration of the BBB. Biodistribution experiments in mice showed high initial uptake into the brain (8.12% and 5.29% ID/g at 2 min, respectively) and fast washout kinetics from the healthy brain (3.04% and 2.12% ID/g at 60 min, respectively), which is highly desirable for Aβ imaging agents. The brain$_{2\ min}$/brain$_{60\ min}$ ratio as an index to compare washout rates is used for determining radioactivity pharmacokinetics in vivo. As shown in Table 4, the brain$_{2\ min}$/brain$_{60\ min}$ ratio of [^{18}F]**24** and [^{18}F]**32** was 2.67 and 2.50, respectively, indicating that [^{18}F]**24** with a monomethylamino group provided the best profile of radioactivity in the brain, and the pharmacokinetics in vivo were improved by changing the dimethylamino group in [^{18}F]**32** to a monomethylamino group. This may be due to the lower lipophilicity of [^{18}F]**24** than [^{18}F]**32** (log *D* = 3.09 and 3.45, respectively). In addition, no marked uptake of [^{18}F]**24** and [^{18}F]**32** in bone was observed (5.78% and 3.45% ID/g at 60 min, respectively), suggesting little defluorination in vivo, and interference with the imaging is expected to be relatively minor.

dx.doi.org/10.1021/jm300251n | J. Med. Chem. 2012, 55, 9136−9145

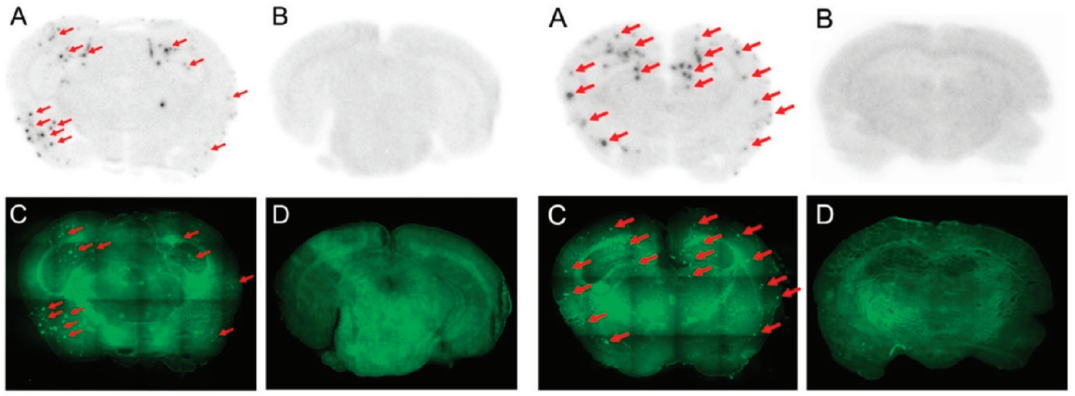

Figure 5. Autoradiography of [^{18}F]**24** (left) and [^{18}F]**32** (right) ex vivo using Tg2576 mice (C57BL6, APPsw, 18 months old) and wild-type controls (C57BL6, 18 months old). Plaques were also confirmed by the staining of the same sections with thioflavin-S.

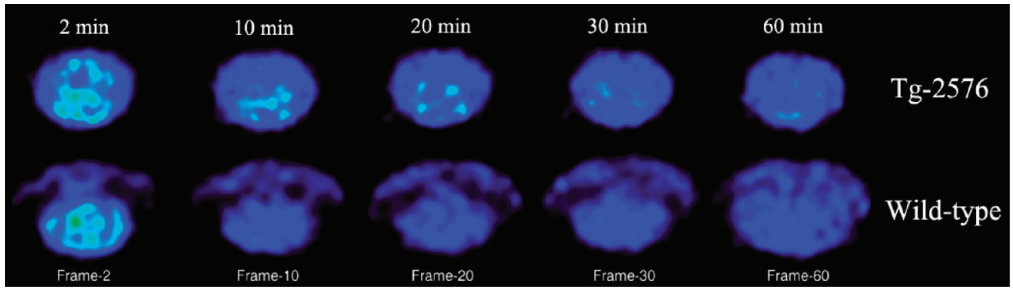

Figure 6. μPET images (coronal views) at 2, 10, 20, 30, and 60 min after injection of [^{18}F]**24** in an aged Tg2576 mouse (C57BL6, APPsw, 31 months old) and aged wild-type mouse (C57BL6, 31 months old).

[^{18}F]**24** and [^{18}F]**32** also distributed to several other organs. The liver and kidneys showed an initial uptake with washout, whereas the intestines showed an accumulation of radioactivity over time. In summary, the initial brain uptake of [^{18}F]**24** (8.12% ID/g) was comparable to the value observed for [^{18}F]**7** (7.33% ID/g),[18] which was just approved by the FDA. Although the brain$_{2\ min}$/brain$_{60\ min}$ ratio of [^{18}F]**24** (2.67) was lower than that of [^{18}F]**7** (3.90), it was improved compared to the values for radiofluoro-pegylated benzofuran and pyridyl-benzofuran derivatives (1.03−2.34).[25] Furthermore, compared with [^{125}I]**12**, the fluoro-pegylated [^{18}F]**24** had greatly improved pharmacokinetics (Table 4).

Ex Vivo Autoradiography of Transgenic Mouse Brain and Wild-Type Mouse Brain. To further characterize the potential of these benzoxazole probes in living mouse brain tissue, ex vivo autoradiography was carried out in Tg2576 mice (C57BL6, APPsw, 18 months old) and wild-type mice (C57BL6, 18 months old). Autoradiography using [^{18}F]**24** or [^{18}F]**32** showed dense labeling of the plaques in the cortical regions and hippocampus of Tg2576 mice (Figure 5A), while wild-type mouse brain showed no such labeling (Figure 5B). Furthermore, the labeling of the plaques with both probes showed a one-to-one correlation with the fluorescent signals obtained with thioflavin S (Figure 5C). The results were comparable to those reported previously for fluorinated benzofuran derivatives.

*Small-Animal PET Studies of [^{18}F]**24** with Tg-2576 and Wild-Type Mice.* Because of the high initial brain uptake of [^{18}F]**24**, this probe with a monomethylamino group was selected for small-animal PET experiments in Tg2576 and wild-type mouse brain. The μPET images and brain uptake kinetics (whole brain) are presented in Figures 6 and 7. After an

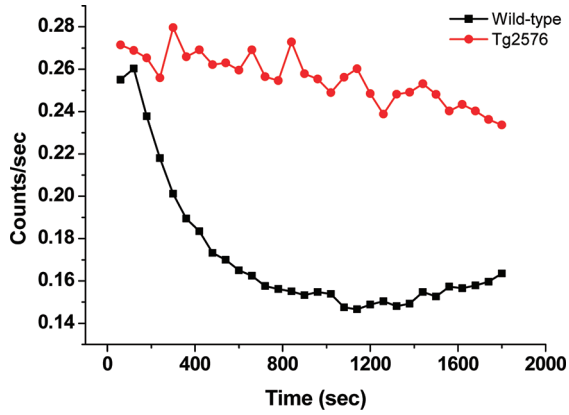

Figure 7. μPET mean TACs of [^{18}F]**24** from brain VOIs in an aged Tg2576 mouse (31 months old) and aged wild-type mouse (31 months old).

intravenous injection, [^{18}F]**24** penetrated the intact BBB efficiently. The brain region displayed a good initial uptake in both Tg2576 and wild-type mice. Because there were no Aβ plaques in the healthy mouse brain, as expected, the radioactivity of [^{18}F]**24** washed out quickly and did not display any specific binding or prolonged retention. In Tg2576 mice, however, the cortices and hippocampus, areas known to contain high concentrations of Aβ plaques, retained the radioactivity of [^{18}F]**24** to a greater extent during the later time points (Figure 6), and we can conclude that [^{18}F]**24** specifically binds to Aβ plaques in the brain of Tg2576 mice. A comparison of time−activity curves based on VOI analyses in mouse brain (Figure 7), revealed significant differences in the clearance profile after the administration of [^{18}F]**24** between Tg2576 and wild-type

dx.doi.org/10.1021/jm300251n | J. Med. Chem. 2012, 55, 9136−9145

mice. The brain$_{2\ min}$/brain$_{20\ min}$ ratio of [^{18}F]**24** was lower in Tg2576 mice (1.21) than wild-type mice (1.77).

CONCLUSION

The present results showed that [^{18}F]**24**, a novel radiofluoropegylated phenylbenzoxazole derivative, has several favorable properties: high affinity for Aβ aggregates (K_i = 9.3 nM); easily labeled with ^{18}F for imaging (radiochemical yield of 30%, which is suitable for commercial scale production and distribution; small (MW < 500), lipophilic (measured log D = 3.09), and neutral; good initial brain uptake and fast washout (8.12% ID/g at 2 min and 3.04% ID/g at 60 min after iv injection)); lower nonspecific binding in white matter as demonstrated by autoradiography in vitro and ex vivo using post-mortem AD brain sections and Tg2576 mice. These findings suggest that [^{18}F]**24** should be investigated further as a potential PET tracer for imaging Aβ plaques in living brain tissue.

EXPERIMENTAL SECTION

General Remarks. All reagents used for chemical synthesis were commercial products and were used without further purification. The ^{1}H NMR spectra were obtained at 400 MHz on JEOL JNM-AL400 NMR spectrometers in $CDCl_3$ solutions at room temperature with TMS as an internal standard. Chemical shifts are reported as δ values relative to the internal TMS. Coupling constants are reported in hertz. Multiplicity is defined by s (singlet), d (doublet), t (triplet), and m (multiplet). Mass spectra were acquired with a Shimadzu GC-MS-QP2010 Plus (ESI). HPLC was performed with a Shimadzu system (a LC-20AT pump with a SPD-20A UV detector, λ = 254 nm) using a column of Cosmosil C18 (Nacalai Tesque, 5C$_{18}$-AR-II, 4.6 mm × 150 mm or 10 mm × 150 mm) and acetonitrile/water as the mobile phase. Fluorescence was observed with a Nikon Eclipse 80i microscope equipped with a BV-2A filter set (excitation, 400−440 nm; diachronic mirror, 455 nm; long pass filter, 470 nm). Purity of the synthesized compounds was determined using analytical HPLC and was found to be more than 95%. ddY Mice (five weeks, male) were used for biodistribution experiments. Transgenic mice (Tg2576, C57BL6, APPsw), used as an Alzheimer's model, were purchased from Taconic Farms, Inc. All protocols requiring the use of mice were approved by the animal care committee of Kyoto University. Post-mortem brain tissues from an autopsy-confirmed case of AD (a 93-year-old, female) and a control (a 71-year-old, male) were obtained from the Graduate School of Medicine, Kyoto University, and BioChain Institute Inc., respectively. Experiments were performed according to the regulations of the ethics committee of Kyoto University.

Chemistry. *2-Amino-4-methoxyphenol (**19**).* A mixture of **18** (5.1 g, 40 mmol) and Pd/C (10%, 0.5 g) in absolute methanol (200 mL) under a hydrogen atmosphere (balloon) was strongly stirred for 24 h at room temperature. The mixture was filtered, and the filtrate washed with methanol (20 mL) and concentrated in vacuo to give **19** (3.72 g, 89.2%).

*4-(5-Methoxybenzo[d]oxazol-2-yl)-N-methylaniline (**20**).* To a mixture of **19** (1.39 g, 10 mmol) and 4-methylaminobenzoic acid (1.51 g, 10 mmol) was added polyphosphoric acid (10 g). The mixture was stirred at 180 °C for 30 min, and after ice water (400 mL) was added, neutralized by K_2CO_3. The mixture was extracted with ethyl acetate (200 mL), and the organic phase was separated and dried over Na_2SO_4. After the solvent was removed, the residue was purified by silica gel chromatography to afford **20** (783 mg, 30.8%). ^{1}H NMR (400 MHz, CD_3OD) δ 7.94 (d, J = 9.0 Hz, 2H), 7.44 (d, J = 8.7 Hz, 1H), 7.12 (d, J = 2.4 Hz, 1H), 6.89 (dd, J = 8.9, 2.6 Hz, 1H), 6.69 (d, J = 8.9 Hz, 2H), 3.84 (s, 3H), 2.85 (s, 3H). MS(ESI): m/z calcd for $C_{15}H_{14}N_2O_2$ 254.11; found 255.10 (M + H$^+$).

*2-(4-(Methylamino)phenyl)benzo[d]oxazol-5-ol (**21**).* To a solution of **20** (510 mg, 2 mmol) was added BBr_3 (1 M in CH_2Cl_2, 10 mL) dropwise in a dry ice−acetone bath. The reaction mixture was stirred for 1 h at −78 °C and an additional 12 h at room temperature, and after ice water (50 mL) was added, neutralized by K_2CO_3. The mixture was extracted with $CHCl_3$ (100 mL), the organic phase was separated, dried over Na_2SO_4, and filtered, and the residue was purified by silica gel chromatography to give **21** (437 mg, 91.1%). ^{1}H NMR (400 MHz, CD_3OD) δ 7.93 (d, J = 8.8 Hz, 2H), 7.37 (d, J = 8.8 Hz, 1H), 6.99 (d, J = 2.1 Hz, 1H), 6.77 (dd, J = 8.7, 2.4 Hz, 1H), 6.69 (d, J = 8.8 Hz, 2H), 2.85 (s, 3H). MS(ESI): m/z calcd for $C_{14}H_{12}N_2O_2$ 240.09; found 241.10 (M + H$^+$).

*2-(2-(2-((2-(4-(Methylamino)phenyl)benzo[d]oxazol-5-yl)oxy)-ethoxy)ethoxy)ethanol (**22**).* To a solution of **21** (480 mg, 2 mmol) and 2-[2-(2-chloroethoxy)-ethoxy]ethanol (50 μL, 0.66 mmol) in DMF (15 mL) was added anhydrous K_2CO_3 (830 mg, 6 mmol). The reaction mixture was stirred for 4 h at 105 °C and then poured into water and extracted with $CHCl_3$. The organic layers were combined and dried over Na_2SO_4. Evaporation of the solvent afforded a residue, which was purified by silica gel chromatography to give **22** (550 mg, 73.9%). ^{1}H NMR (400 MHz, $CDCl_3$) δ 8.05 (d, J = 8.3 Hz, 2H), 7.38 (d, J = 8.8 Hz, 1H), 7.28 (d, J = 2.4 Hz, 1H), 6.90 (dd, J = 8.8, 2.5 Hz, 1H), 6.67 (d, J = 8.4 Hz, 2H), 4.24−4.14 (m, 2H), 3.91−3.86 (m, 2H), 3.79−3.68 (m, 6H), 3.67−3.61 (m, 2H), 2.92 (s, 3H). MS(ESI): m/z calcd for $C_{20}H_{24}N_2O_5$ 372.17; found 373.15 (M + H$^+$).

*N-Methyl-4-(5-((2,2,3,3-tetramethyl-4,7,10-trioxa-3-siladodecan-12-yl)oxy)benzo[d]oxazol-2-yl)aniline (**23**).* A solution of **22** (372 mg, 1 mmol), TBDMSCl (226 mg, 1.5 mmol), and imidazole (140 mg, 2 mmol) in dichloromethane (10 mL) was stirred at room temperature for 3 h. A white solid formed and was filtered off. After the filtrate was evaporated, the residue was purified by silica gel column chromatography to afford **23** (302 mg, 62.1%). ^{1}H NMR (400 MHz, $CDCl_3$) δ 7.96 (d, J = 8.6 Hz, 2H), 7.30 (d, J = 8.8 Hz, 1H), 7.14 (d, J = 2.5 Hz, 1H), 6.82 (dd, J = 8.8, 2.4 Hz, 1H), 6.58 (d, J = 8.7 Hz, 2H), 4.22 (s, 1H), 4.13−4.04 (m, 2H), 3.84−3.79 (m, 2H), 3.71 (t, J = 5.4 Hz, 2H), 3.69−3.61 (m, 4H), 3.51 (t, J = 5.4 Hz, 2H), 2.81 (s, 3H), 0.83 (s, 9H). MS(ESI): m/z calcd for $C_{26}H_{38}N_2O_5Si$ 486.25; found 487.30 (M + H$^+$).

*4-(5-(2-(2-(2-Fluoroethoxy)ethoxy)ethoxy)benzo[d]oxazol-2-yl)-N-methylaniline (**24**).* To a solution of **22** (74 mg, 0.2 mmol) in $CHCl_3$ (10 mL) was added DAST (100 mg, 0.6 mmol) in a dry ice−acetone bath. The reaction mixture was stirred for 2 h at room temperature and then poured into a saturated $NaHSO_3$ solution and extracted with $CHCl_3$. The organic phase was separated, dried over $MgSO_4$, and filtered, and the residue was purified by silica gel chromatography to give **24** (7.1 mg, 9.6%). ^{1}H NMR (400 MHz, $CDCl_3$) δ 8.04 (d, J = 8.5 Hz, 2H), 7.38 (d, J = 8.8 Hz, 1H), 7.21 (d, J = 2.5 Hz, 1H), 6.89 (dd, J = 8.8, 2.5 Hz, 1H), 6.67 (d, J = 8.6 Hz, 2H), 4.63 (dd, J = 4.5, 3.9 Hz, 1H), 4.51 (dd, J = 6.0, 2.3 Hz, 1H), 4.23−4.13 (m, 2H), 3.95−3.86 (m, 2H), 3.84−3.79 (m, 2H), 3.78−3.71 (m, 4H), 2.92 (s, 3H). HRMS(EI): m/z calcd for $C_{20}H_{23}FN_2O_4$ 374.1642; found 374.1637 (M + H$^+$).

*tert-Butyl Methyl(4-(5-((2,2,3,3-tetramethyl-4,7,10-trioxa-3-sila-dodecan-12-yl)oxy)benzo[d]oxazol-2-yl)phenyl)carbamate (**25**).* Under a nitrogen atmosphere, **23** (300 mg, 0.62 mmol) was dissolved in anhydrous tetrahydrofuran (THF) (20 mL) followed by Boc-anhydride (1.35 g, 6.2 mmol). The solution was refluxed for 48 h. After the reaction was complete, the solvent was removed and the residue was purified by silica gel column chromatography to afford **25** (273 mg, 74.7%). ^{1}H NMR (400 MHz, $CDCl_3$) δ 8.11 (d, J = 8.4 Hz, 2H), 7.37 (d, J = 8.8 Hz, 1H), 7.35 (d, J = 8.5 Hz, 2H), 7.19 (d, J = 2.5 Hz, 1H), 6.91 (dd, J = 8.8, 2.5 Hz, 1H), 4.19−4.09 (m, 2H), 3.88−3.80 (m, 2H), 3.71 (t, J = 5.4 Hz, 2H), 3.69−3.61 (m, 4H), 3.51 (dd, J = 5.6, 5.1 Hz, 2H), 3.26 (s, 3H), 1.42 (s, 9H), 0.83 (s, 9H). MS(ESI): m/z calcd for $C_{31}H_{46}N_2O_7Si$ 586.31; found 587.40 (M + H$^+$).

*tert-Butyl (4-(5-(2-(2-(2-Hydroxyethoxy)ethoxy)ethoxy)benzo[d]-oxazol-2-yl)phenyl)(methyl)carbamate (**26**).* To a solution of **25** (270 mg, 0.46 mmol) in dry THF (10 mL) was added anhydrous TBAF (1.0 mL, 1 M in THF). The solution was stirred at room temperature for 2 h. After removal of the THF, the residue was purified by silica gel chromatography to give **26** (281 mg, 75.7%). ^{1}H NMR (400 MHz, $CDCl_3$) δ 8.09 (d, J = 8.8 Hz, 2H), 7.39−7.30 (m, 3H), 7.22 (s, 1H), 6.90 (d, J = 8.8 Hz, 1H), 4.11 (dd, J = 6.2, 2.9 Hz, 2H), 3.88−3.75 (m, 2H), 3.70−3.60 (m, 6H), 3.58−3.51 (m, 2H),

dx.doi.org/10.1021/jm300251n | J. Med. Chem. 2012, 55, 9136−9145

3.24 (s, 3H), 1.41 (s, 9H). MS(ESI): m/z calcd for $C_{25}H_{32}N_2O_7$ 472.22; found 473.30 (M + H$^+$).

*2-(2-(2-((2-(4-((tert-Butoxycarbonyl)(methyl)amino)phenyl)-benzo[d]oxazol-5-yl)oxy)ethoxy)ethoxy)ethyl methanesulfonate (**27**).* To a solution of **26** (281 mg, 0.6 mmol) in dichloromethane (10 mL) was added triethylamine (121 mg, 1.2 mmol). Methanesulfonyl chloride (137 mg, 1.2 mmol) was then added via a syringe. The solution was stirred at room temperature for 2 h. Next, 20 mL of water was added and the solution was extracted with $CHCl_3$. The organic layer was dried over $MgSO_4$. After the solvent was removed, the residue was purified by silica gel chromatography to afford **27** (173 mg, 52.4%). ^{1}H NMR (400 MHz, $CDCl_3$) δ 8.17 (d, J = 8.7 Hz, 2H), 7.45 (d, J = 8.9 Hz, 1H), 7.42 (d, J = 8.7 Hz, 2H), 7.25 (d, J = 2.5 Hz, 1H), 6.97 (dd, J = 8.9, 2.5 Hz, 1H), 4.42−4.35 (m, 2H), 4.21−4.14 (m, 2H), 3.88 (dd, J = 5.3, 4.0 Hz, 2H), 3.81−3.77 (m, 2H), 3.76−3.69 (m, 4H), 3.33 (s, 3H), 3.06 (s, 3H), 1.49 (s, 9H). MS(ESI): m/z calcd for $C_{26}H_{34}N_2O_9S$ 550.20; found 551.25 (M + H$^+$).

*4-(5-Methoxybenzo[d]oxazol-2-yl)-N,N-dimethylaniline (**28**).* To a mixture of **19** (1.39 g, 10 mmol) and 4-(dimethylamino)benzoic acid (1.65 g, 10 mmol) was added polyphosphoric acid (30 g). The mixture was stirred at 180 °C for 30 min, and after ice water (400 mL) was added, neutralized by K_2CO_3. The mixture was extracted with ethyl acetate (200 mL), and the organic phase was separated and dried over Na_2SO_4. After the solvent was removed, the residue was purified by silica gel chromatography to afford **28** (672 mg, 25.1%). ^{1}H NMR (400 MHz, $CDCl_3$) δ 8.08 (d, J = 8.7 Hz, 2H), 7.39 (d, J = 8.8 Hz, 1H), 7.21 (d, J = 2.5 Hz, 1H), 6.86 (dd, J = 8.8, 2.5 Hz, 1H), 6.77 (d, J = 8.9 Hz, 2H), 3.86 (s, 3H), 3.07 (s, 3H). MS(ESI): m/z calcd for $C_{16}H_{16}N_2O_2$ 268.12; found 269.15 (M + H$^+$).

*2-(4-(Dimethylamino)phenyl)benzo[d]oxazol-5-ol (**29**).* To a solution of **28** (536 mg, 2 mmol) was added BBr_3 (1 M in CH_2Cl_2, 10 mL) dropwise in a dry ice−acetone bath. The reaction mixture was stirred for 1 h at −78 °C and an additional 12 h at room temperature, and after ice water (50 mL) was added, neutralized by K_2CO_3. The mixture was extracted with $CHCl_3$ (100 mL), the organic phase was separated, dried over Na_2SO_4, and filtered, and the residue was purified by silica gel chromatography to give **29** (447 mg, 88.0%). ^{1}H NMR (400 MHz, CD_3OD) δ 7.99 (d, J = 8.9 Hz, 2H), 7.38 (d, J = 8.7 Hz, 1H), 7.00 (d, J = 2.4 Hz, 1H), 6.84 (d, J = 8.9 Hz, 2H), 6.78 (ddd, J = 8.8, 2.4, 0.8 Hz, 1H), 3.07 (s, 6H). MS(ESI): m/z calcd for $C_{15}H_{14}N_2O_2$ 254.11; found 255.10 (M + H$^+$).

*2-(2-(2-((2-(4-(Dimethylamino)phenyl)benzo[d]oxazol-5-yl)oxy)-ethoxy)ethoxy)ethanol (**30**).* To a solution of **29** (380 mg, 1.5 mmol) and 2-[2-(2-chloroethoxy)-ethoxy]ethanol (510 mg, 3 mmol) in DMF (10 mL) was added anhydrous K_2CO_3 (280 mg, 2 mmol). The reaction mixture was stirred for 3 h at 110 °C and then poured into water and extracted with $CHCl_3$. The organic layers were combined and dried over Na_2SO_4. Evaporation of the solvent afforded a residue, which was purified by silica gel chromatography to give **30** (250 mg, 43.1%). ^{1}H NMR (400 MHz, $CDCl_3$) δ 8.05 (d, J = 7.9 Hz, 2H), 7.37 (d, J = 8.8 Hz, 1H), 7.24 (d, J = 2.3 Hz, 1H), 6.88 (dd, J = 8.8, 2.5 Hz, 1H), 6.72 (d, J = 8.2 Hz, 2H), 4.17 (dd, J = 4.9, 3.8 Hz, 2H), 3.86 (dd, J = 4.9, 3.8 Hz, 2H), 3.78−3.42 (m, 8H), 3.02 (s, 6H). MS(ESI): m/z calcd for $C_{21}H_{26}N_2O_5$ 386.18; found 387.27 (M + H$^+$).

*2-(2-(2-((2-(4-(Dimethylamino)phenyl)benzo[d]oxazol-5-yl)oxy)-ethoxy)ethoxy)ethyl 4-Methylbenzenesulfonate (**31**).* To a solution of **30** (250 mg, 0.65 mmol) in pyridine (10 mL) was added tosyl chloride (248 mg, 1.30 mmol). The reaction mixture was stirred for 3 h at room temperature, 50 mL of water was added, and the mixture was extracted with $CHCl_3$. The organic layer was dried over Na_2SO_4, and evaporation of the solvent afforded a residue, which was purified by silica gel chromatography to give **31** (150 mg, 42.7%). ^{1}H NMR (400 MHz, $CDCl_3$) δ 8.06 (d, J = 9.0 Hz, 2H), 7.79 (d, J = 8.3 Hz, 2H), 7.37 (d, J = 8.8 Hz, 1H), 7.31 (d, J = 8.0 Hz, 2H), 7.19 (d, J = 2.5 Hz, 1H), 6.87 (dd, J = 8.8, 2.5 Hz, 1H), 6.74 (d, J = 9.1 Hz, 2H), 4.20−4.11 (m, 4H), 3.88−3.81 (m, 2H), 3.74−3.56 (m, 6H), 3.04 (s, 6H), 2.40 (s, 3H). MS(ESI): m/z calcd for $C_{28}H_{32}N_2O_7S$ 540.19; found 541.29 (M + H$^+$).

*4-(5-(2-(2-(2-Fluoroethoxy)ethoxy)ethoxy)benzo[d]oxazol-2-yl)-N,N-dimethylaniline (**32**).* To a solution of **31** (54 mg, 0.1 mmol) in 10 mL of dry tetrahydrofuran (THF) was added anhydrous TBAF (300 μL, 1 M in THF). The reaction mixture was refluxed for 3 h. After removal of the THF, the residue was purified by silica gel chromatography to give **32** (22 mg, 56.7%). ^{1}H NMR (400 MHz, $CDCl_3$) δ 8.08 (d, J = 9.0 Hz, 2H), 7.38 (d, J = 8.8 Hz, 1H), 7.21 (d, J = 2.5 Hz, 1H), 6.89 (dd, J = 8.8, 2.5 Hz, 1H), 6.77 (d, J = 9.1 Hz, 2H), 4.67−4.59 (m, 1H), 4.55−4.45 (m, 1H), 4.24−4.14 (m, 2H), 3.93−3.85 (m, 2H), 3.84−3.65 (m, 6H), 3.07 (s, 6H). HRMS(EI): m/z calcd for $C_{21}H_{25}FN_2O_4$ 388.1798; found 388.1805 (M + H$^+$).

Radiosynthesis. [^{18}F]Fluoride trapped on an anion exchange cartridge was eluted with a K_2CO_3 solution (33 mM). Kryptofix$_{222}$ (6−8 mg) was dissolved in the solution of [^{18}F]fluoride in water. The solvent was removed at 120 °C under a stream of nitrogen gas. The residue was azeotropically dried with 0.3 mL of anhydrous acetonitrile twice at 120 °C under a stream of nitrogen gas.

For [^{18}F]**24**, a solution of the mesylate precursor **27** (1.0 mg) in CH_3CN (0.2 mL) was added to the reaction vessel containing the $^{18}F^-$ activity. The mixture was heated at 120 °C for 6 min. After the solution had cooled to room temperature, HCl (1 M aqueous solution, 0.2 mL) was added and the mixture was heated at 120 °C again for 5 min. An aqueous solution of K_2CO_3 was added to adjust the pH to basic (pH 8−9). Water (5 mL) was added, and the mixture was passed through a preconditioned Sep-Pak Plus PS-2 cartridge (Waters). The cartridge was washed with 20 mL of water, and the labeled compound was eluted with 3 mL of acetonitrile. After the solvent was removed, the residue was dissolved in CH_3CN and subjected to HPLC for purification (Nacalai Tesque, 5C18-AR-II, 4.6 mm × 150 mm, CH_3CN/water = 1/1; flow rate = 1 mL/min). The retention time of [^{18}F]**24** was 8.22 min in this HPLC system. The preparation took 60 min, and the radiochemical yield was 30% (decay corrected).

For [^{18}F]**32**, a solution of the tosylate precursor **31** (1.0 mg) in CH_3CN (0.2 mL) was added to the reaction vessel containing the $^{18}F^-$ activity. The mixture was heated at 120 °C for 6 min. Water (5 mL) was added, and the mixture was passed through a preconditioned Sep-Pak Plus PS-2 cartridge (Waters). The cartridge was washed with 20 mL of water, and the labeled compound was eluted with 3 mL of acetonitrile. The eluted compound was purified by HPLC (Nacalai Tesque, 5C18-AR-II, 4.6 mm × 150 mm). The retention time of [^{18}F]**32** was 7.55 min in this HPLC system (CH_3CN/water = 6/4; flow rate = 1 mL/min). The preparation took 40 min and the radiochemical yield was 60% (decay corrected). The radiochemical purity of both tracers was greater than 98%.

In Vitro Binding Studies of 24 and 32. Inhibition experiments were carried out in 12 mm × 75 mm borosilicate glass tubes according to procedures described previously with some modifications.[25,30] Briefly, 100 μL of aggregated Aβ fibrils (60 nM in the final assay mixture) was added to a mixture containing 100 μL of radioligands ([^{125}I]IMPY) at an appropriate concentration, 10 μL of inhibitors (10^{-5}−10^{-10} M in ethanol), and 790 μL of PBS (0.2 M, pH = 7.4) in a final volume of 1 mL. Nonspecific binding was defined in the presence of 1 μM IMPY. The mixture was incubated for 2 h at 37 °C with constant shaking, and then the bound and free radioactive fractions were separated by vacuum filtration through borosilicate glass fiber filters (Whatman GF/B) using a M-24 cell harvester (Brandel, Gaithersburg, MD). The radioactivity from filters containing the bound ^{125}I ligand was measured in a γ-counter (WALLAC/Wizard 1470, USA) with 70% efficiency. Under the assay conditions, the specifically bound fraction accounted for about 10% of total radioactivity. The half-maximal inhibitory concentration (IC_{50}) was determined using GraphPad Prism 4.0, and the inhibition constant (K_i) was calculated using the Cheng−Prusoff equation: $K_i = IC_{50}/(1 + [L]/K_d)$.[31]

Measurement of Partition Coefficient. [^{18}F]**24** or [^{18}F]**32** (370 kBq) was added to a premixed suspension containing 3 g of n-octanol and 3 g of PBS (0.05 M, pH = 7.4) in a test tube. The test tube was vortexed for 3 min at room temperature and centrifuged for 5 min at 3000 rpm. Two weighed samples from the n-octanol (100 μL) and buffer (500 μL) layers were measured. The partition coefficient was expressed as the logarithm of the ratio of the count per gram from n-octanol versus PBS. Samples from the n-octanol layer were

repartitioned until consistent partition coefficient values were obtained. The measurement was done in triplicate and repeated three times.

In Vitro Autoradiography of Transgenic Mouse Brain Sections and AD Brain Sections. Paraffin-embedded mouse brain sections (Tg mouse, C57BL6, APPswe/PSEN1, 12 months old; wild-type, C57BL6, 12 months old) and human brain sections (AD, 93 years old, female; normal, 71 years old, male) were deparaffinized with 2 × 20 min washes in xylene, 2 × 5 min washes in 100% ethanol, a 5 min wash in 90% ethanol/H_2O, a 5 min wash in 80% ethanol/H_2O, a 5 min wash in 60% ethanol/H_2O, and a 10 min wash in running tap water and then incubated in PBS (0.2 M, pH = 7.4) for 30 min. The sections were incubated with [^{18}F]**24** or [^{18}F]**32** (370 kBq/100 μL) for 1 h at room temperature, washed with 50% ethanol for 1 min, and rinsed with water for 1 min. After drying, the labeled sections were exposed to a Fuji Film imaging plate overnight. The in vitro autoradiographic images were obtained using a BAS5000 scanner system (Fuji Film). The presence and location of plaques in the sections were confirmed with fluorescent staining using thioflavin S or immunohistochemical staining using a monoclonal Aβ_{1-42} antibody, BC05 (Wako Pure Chemical Inc., Osaka, Japan).

In Vivo Biodistribution in Normal ddY Mice. Normal male ddY mice (5 weeks, 20−22 g, n = 5) were injected with [^{18}F]**24** or [^{18}F]**32** (370 kBq/100 μL saline containing 5% EtOH) directly into a tail vein. The mice were sacrificed at various time points postinjection. The organs of interest were removed and weighed, and the radioactivity was measured with an automatic γ-counter (WALLAC/Wizard 1470, USA). The percent dose per gram of wet tissue was calculated by a comparison of the tissue counts to suitably diluted aliquots of the injected material.

Ex Vivo Autoradiography of Transgenic Mouse Brain and Wild-Type Mouse Brain. Autoradiography was performed using Tg2576 (C57BL6, APPsw, 18 months old) and wild-type (C57BL6, 18 months old) mice. A saline solution (100 μL, 5% EtOH) of 40.7 MBq of [^{18}F]**24** or [^{18}F]**32** was injected iv through the femoral vein, and the animals were sacrificed by decapitation 30 min later. The brains were removed and frozen in powdered dry ice immediately. Sections of 20 μm were cut and exposed to a BAS imaging plate (Fuji Film, Tokyo, Japan) for 8 h. Autoradiographic images were obtained using a BAS5000 scanner system (Fuji Film). After the autoradiographic examination, the presence of amyloid plaques was confirmed by staining the same sections with thioflavin-S in vitro.

μPET Studies of [^{18}F]24 in Transgenic and Wild-Type Mice. A female Tg2576 mouse (C57BL6, APPsw, 31 months old) and a female wild-type mouse (C57BL6, 31 months old) were anesthetized with isoflurane (1.5−2.5%) in oxygen at a flow rate of 1−2 L/min and injected with 40.7 MBq of [^{18}F]**24** (100 μL, 5% EtOH) via a tail vein. Dynamic μPET images were acquired for 60 min, and reconstruction was done using filtered back projection with a RAMP filter. Data were analyzed using PMOD software, volumes of interest (VOIs) were defined on the summed images, and time−activity curves (TACs) were drawn.

■ ASSOCIATED CONTENT

Ⓢ Supporting Information

HPLC chromatograms of **24**, **32**, [^{18}F]**24**, and [^{18}F]**32**. This material is available free of charge via the Internet at http://pubs.acs.org.

■ AUTHOR INFORMATION

Corresponding Author

*Phone: +81-75-753-4608. Fax: +81-75-753-4568. E-mail: ono@pharm.kyoto-u.ac.jp.

Notes

The authors declare no competing financial interest.

■ ACKNOWLEDGMENTS

This study was supported by the Funding Program for Next Generation World-Leading Researchers (NEXT Program) from the Japan Society for the Promotion of Science (JSPS) and the China Scholarship Council (CSC).

■ ABBREVIATIONS USED

AD, Alzheimer's disease; Aβ, β-amyloid; NFTs, neurofibrillary tangles; PET, positron emission tomography; PEG, polyethylene glycol; BBB, blood−brain barrier; TBDMSCl, *tert*-butyldimethylsilyl chloride; BOC, butyloxycarbonyl; HPLC, high performance liquid chromatography; THF, tetrahydrofuran; TBAF, tetra-*n*-butylammonium fluoride; DAST, diethylaminosulfur trifluoride; Tg, transgenic

■ REFERENCES

(1) Selkoe, D. J. The origins of Alzheimer disease: A is for amyloid. *JAMA, J. Am. Med. Assoc.* **2000**, *283*, 1615−1617.
(2) Selkoe, D. J. Alzheimer's disease: genes, proteins, and therapy. *Physiol. Rev.* **2001**, *81*, 741−766.
(3) Hardy, J. A.; Selkoe, D. J. The amyloid hypothesis of Alzheimer's disease: progress and problems on the road to therapeutics. *Science* **2002**, *297*, 353−356.
(4) Kung, H. F.; Choi, S. R.; Qu, W. C.; Zhang, W.; Skovronsky, D. F-18 Stilbenes and styrylpyridines for PET imaging of Aβ plaques in Alzheimer's disease: a miniperspective. *J. Med. Chem.* **2010**, *53*, 933−941.
(5) Mathis, C. A.; Wang, Y.; Klunk, W. E. Imaging β-amyloid plaques and neurofibrillary tangles in the aging human brain. *Curr. Pharm. Des.* **2004**, *10*, 1469−1492.
(6) Herholz, K.; Ebmeier, K. Clinical amyloid imaging in Alzheimer's disease. *Lancet Neurol.* **2011**, *10*, 667−670.
(7) Mathis, C. A.; Wang, Y. M.; Holt, D. P.; Huang, G. F.; Debnath, M. L.; Klunk, W. E. Synthesis and evaluation of C-11-labeled 6-substituted 2-arylbenzothiazoles as amyloid imaging agents. *J. Med. Chem.* **2003**, *46*, 2740−2754.
(8) Klunk, W. E.; Engler, H.; Nordberg, A.; Wang, Y. M.; Blomqvist, G.; Holt, D. P.; Bergstrom, M.; Savitcheva, I.; Huang, G. F.; Estrada, S.; Ausen, B.; Debnath, M. L.; Barletta, J.; Price, J. C.; Sandell, J.; Lopresti, B. J.; Wall, A.; Koivisto, P.; Antoni, G.; Mathis, C. A.; Langstrom, B. Imaging brain amyloid in Alzheimer's disease with Pittsburgh Compound-B. *Ann. Neurol.* **2004**, *55*, 306−319.
(9) Klunk, W. E.; Mathis, C. A.; Price, J. C.; Lopresti, B. J.; DeKosky, S. T. Two-year follow-up of amyloid deposition in patients with Alzheimer's disease. *Brain* **2006**, *129*, 2805−2807.
(10) Johnson, A. E.; Jeppsson, F.; Sandell, J.; Wensbo, D.; Neelissen, J. A. M.; Jureus, A.; Strom, P.; Norman, H.; Farde, L.; Svensson, S. P. S. AZD2184: a radioligand for sensitive detection of β-amyloid deposits. *J. Neurochem.* **2009**, *108*, 1177−1186.
(11) Nyberg, S.; Jonhagen, M. E.; Cselenyi, Z.; Halldin, C.; Julin, P.; Olsson, H.; Freund-Levi, Y.; Andersson, J.; Varnas, K.; Svensson, S.; Farde, L. Detection of amyloid in Alzheimer's disease with positron emission tomography using [C-11]AZD2184. *Eur. J. Nucl. Med. Mol. Imaging* **2009**, *36*, 1859−1863.
(12) Andersson, J. D.; Varnas, H.; Cselenyi, Z.; Gulyas, B.; Wensbo, D.; Finnema, S. J.; Swahn, B. M.; Svensson, S.; Nyberg, S.; Farde, L.; Halldin, C. Radiosynthesis of the candidate β-amyloid radioligand [C-11]AZD2184: positron emission tomography examination and metabolite analysis in cynomolgus monkeys. *Synapse* **2010**, *64*, 733−741.
(13) Ono, M.; Wilson, A.; Nobrega, J.; Westaway, D.; Verhoeff, P.; Zhuang, Z. P.; Kung, M. P.; Kung, H. F. C-11-labeled stilbene derivatives as Aβ-aggregate-specific PET imaging agents for Alzheimer's disease. *Nucl. Med. Biol.* **2003**, *30*, 565−571.
(14) Verhoeff, N. P. L. G.; Wilson, A. A.; Takeshita, S.; Trop, L.; Hussey, D.; Singh, K.; Kung, H. F.; Kung, M. P.; Houle, S. In vivo

imaging of Alzheimer disease β-amyloid with [C-11]SB-13 PET. *Am. J. Geriatr. Psychiatry* **2004**, *12*, 584−595.
(15) Koole, M.; Lewis, D. M.; Buckley, C.; Nelissen, N.; Vandenbulcke, M.; Brooks, D. J.; Vandenberghe, R.; Van Laere, K. Whole-body biodistribution and radiation dosimetry of F-18-GE067: a radioligand for in vivo brain amyloid imaging. *J. Nucl. Med.* **2009**, *50*, 818−822.
(16) Jureus, A.; Swahn, B. M.; Sandell, J.; Jeppsson, F.; Johnson, A. E.; Johnstrom, P.; Neelissen, J. A.; Sunnemark, D.; Farde, L.; Svensson, S. P. Characterization of AZD4694, a novel fluorinated Aβ plaque neuroimaging PET radioligand. *J. Neurochem.* **2010**, *114*, 784−794.
(17) Rowe, C. C.; Ackerman, U.; Browne, W.; Mulligan, R.; Pike, K. L.; O'Keefe, G.; Tochon-Danguy, H.; Chan, G.; Berlangieri, S. U.; Jones, G.; Dickinson-Rowe, K. L.; Kung, H. P.; Zhang, W.; Kung, M. P.; Skovronsky, D.; Dyrks, T.; Hall, G.; Krause, S.; Friebe, M.; Lehman, L.; Lindemann, S.; Dinkelborg, L. M.; Masters, C. L.; Villemagne, V. L. Imaging of amyloid β in Alzheimer's disease with F-18-BAY94−9172, a novel PET tracer: proof of mechanism. *Lancet Neurol.* **2008**, *7*, 129−135.
(18) Choi, S. R.; Golding, G.; Zhuang, Z. P.; Zhang, W.; Lim, N.; Hefti, F.; Benedum, T. E.; Kilbourn, M. R.; Skovronsky, D.; Kung, H. F. Preclinical properties of F-18-AV-45: a PET agent for Aβ plaques in the brain. *J. Nucl. Med.* **2009**, *50*, 1887−1894.
(19) Lin, K. J.; Hsu, W. C.; Hsiao, I. T.; Wey, S. P.; Jin, L. W.; Skovronsky, D.; Wai, Y. Y.; Chang, H. P.; Lo, C. W.; Yao, C. H.; Yen, T. C.; Kung, M. P. Whole-body biodistribution and brain PET imaging with [F-18]AV-45, a novel amyloid imaging agent—a pilot study. *Nucl. Med. Biol.* **2010**, *37*, 497−508.
(20) Wong, D. F.; Rosenberg, P. B.; Zhou, Y.; Kumar, A.; Raymont, V.; Ravert, H. T.; Dannals, R. F.; Nandi, A.; Brasic, J. R.; Ye, W. G.; Hilton, J.; Lyketsos, C.; Kung, H. F.; Joshi, A. D.; Skovronsky, D. M.; Pontecorvo, M. J. In vivo imaging of amyloid deposition in Alzheimer disease using the radioligand F-18-AV-45 (Flobetapir F 18). *J. Nucl. Med.* **2010**, *51*, 913−920.
(21) Ono, M.; Kung, M. P.; Hou, C.; Kung, H. F. Benzofuran derivatives as Aβ-aggregate-specific imaging agents for Alzheimer's disease. *Nucl. Med. Biol.* **2002**, *29*, 633−642.
(22) Ono, M.; Kawashima, H.; Nonaka, A.; Kawai, T.; Haratake, M.; Mori, H.; Kung, M. P.; Kung, H. F.; Saji, H.; Nakayama, M. Novel benzofuran derivatives for PET imaging of β-amyloid plaques in Alzheimer's disease brains. *J. Med. Chem.* **2006**, *49*, 2725−2730.
(23) Cheng, Y.; Ono, M.; Kimura, H.; Kagawa, S.; Nishii, R.; Kawashima, H.; Sajio, H. Fluorinated benzofuran derivatives for PET imaging of β-amyloid plaques in Alzheimer's disease brains. *ACS Med. Chem. Lett.* **2010**, *1*, 321−325.
(24) Cheng, Y.; Ono, M.; Kimura, H.; Kagawa, S.; Nishii, R.; Saji, H. A novel F-18-labeled pyridyl benzofuran derivative for imaging of β-amyloid plaques in Alzheimer's brains. *Bioorg. Med. Chem. Lett.* **2010**, *20*, 6141−6144.
(25) Ono, M.; Cheng, Y.; Kimura, H.; Cui, M.; Kagawa, S.; Nishii, R.; Saji, H. Novel ^{18}F-labeled benzofuran derivatives with improved properties for positron emission tomography (PET) imaging of β-amyloid plaques in Alzheimer's brains. *J. Med. Chem.* **2011**, *54*, 2971−2979.
(26) Zhuang, Z. P.; Kung, M. P.; Hou, C.; Plossl, K.; Skovronsky, D.; Gur, T. L.; Trojanowski, J. Q.; Lee, V. M. Y.; Kung, H. F. IBOX(2-(4′-dimethylaminophenyl)-6-iodobenzoxazole): a ligand for imaging amyloid plaques in the brain. *Nucl. Med. Biol.* **2001**, *28*, 887−894.
(27) Kung, M. P.; Hou, C.; Zhuang, Z. P.; Zhang, B.; Skovronsky, D.; Trojanowski, J. Q.; Lee, V. M.; Kung, H. F. IMPY: An improved thioflavin-T derivative for in vivo labeling of β-amyloid plaques. *Brain Res.* **2002**, *956*, 202−210.
(28) Zhuang, Z. P.; Kung, M. P.; Wilson, A.; Lee, C. W.; Plossl, K.; Hou, C.; Holtzman, D. M.; Kung, H. F. Structure−activity relationship of imidazo[1,2-*a*]pyridines as ligands for detecting β-amyloid plaques in the brain. *J. Med. Chem.* **2003**, *46*, 237−243.
(29) Newberg, A. B.; Wintering, N. A.; Plossl, K.; Hochold, J.; Stabin, M. G.; Watson, M.; Skovronsky, D.; Clark, C. M.; Kung, M. P.; Kung, H. F. Safety, biodistribution, and dosimetry of ^{123}I-IMPY: a novel amyloid plaque-imaging agent for the diagnosis of Alzheimer's disease. *J. Nucl. Med.* **2006**, *47*, 748−754.
(30) Kung, M. P.; Hou, C.; Zhuang, Z. P.; Zhang, B.; Skovronsky, D.; Trojanowski, J. Q.; Lee, V. M. Y.; Kung, H. F. IMPY: an improved thioflavin-T derivative for in vivo labeling of β-amyloid plaques. *Brain Res.* **2002**, *956*, 202−210.
(31) Cheng, Y.; Prusoff, W. H. Relationship between the inhibition constant (K_i) and the concentration of inhibitor which causes 50% inhibition (I_{50}) of an enzymatic reaction. *Biochem. Pharmacol.* **1973**, *22*, 3099−3108.

NOTE ADDED AFTER ASAP PUBLICATION

The version of this paper that was published on the Web June 12, 2012, did not include all final corrections. The corrected version was reposted June 14, 2012.